Weierstraß–Institut
für Angewandte Analysis und Stochastik

Rate dependence of hysteresis in one-dimensional phase transitions

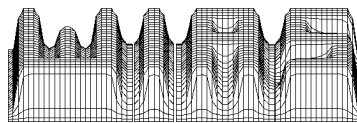Nikolaus Bubner[1], Gail Mackin[2], Robert C. Rogers[3]

submitted: December 13, 1999

[1]   Weierstrass Institute for Applied Analysis and Stochastics,
      Mohrenstr. 39, D–10117 Berlin, Germany
[2]   Department of Mathematics & Computer Science,
      Georgia Southern University,
      Landrum PO Box 8093, Statesboro, GA 30460-8093, USA

[3]   Department of Mathematics, Virginia Tech,
      Blacksburg, VA 24061-0123, USA

Rate dependence of hysteresis in one-dimensional phase transitions

Nikolaus Bubner

Gail Mackin

Department of Mathematics and Computer Science

Georgia Southern University

PO Box 8093

Statesboro, GA 30460-8093

Telephone: (912) 681-5202

Fax: (912) 681-0654

e-mail: mackin@gsu.cs.gasou.edu

Robert C. Rogers*

Virginia Polytechnic Institute and State University

December 2, 1999

Abstract

Two models for solid-solid phase transitions in one-dimension are examined. Thermal dissipation and a rate-type viscosity are added to a stress with strain gradient. Numerical examination of both models reveal similar results, in particular, stress-strain hysteresis, which is a commonly observed phenomena, and stability of single-phase boundary solutions.

PACS-1995: 81.30

Keywords: hysteresis, numerical simulation, rate-type viscosity, solid-solid phase transitions, thermal dissipation.

1 Introduction

In the wake of Ericksen's seminal work [10] there have been many attempts to model solid-solid phase transitions using one-dimensional elasticity. Some representative examples of this work are contained in the following references [1,

2, 4, 5, 9, 12, 6, 19, 20, 21, 22]. In general, these works share the common feature of a nonmonotone stress-strain law while comparing a variety of dissipative mechanisms. These terms serve to regularize the mathematical problem and thus act as physical selection mechanisms that pick out particular solutions from the many that are admitted by the nonmonotone stress-strain law.

In this paper we examine the effects of a higher order gradient term known variously as a couple stress, strain-gradient, Ginzburg, capillarity, or interfacial contribution to the stress. The characterization of solutions of the elastostatic problem with displacement boundary conditions is well understood [9].

- A finite collection of solutions of the balance laws exists. Solutions can have multiple interfaces, but solutions with more than one interface are unstable; the energy of such solutions can be decreased by moving the interface. (Moving the interface is a "small" motion in the natural norm of the problem.)

- The stable solutions are either single phase (no interface) or two phase with one interface and a constant stress on the Maxwell line of the nonconvex stress-strain law.

This last feature, the absence of stress-strain hysteresis, can be considered a defect in a model of solid-solid transitions. Hysteresis is very common in observations of these phenomena and can be quite large (see, e.g. [3, 14]). In this paper we examine the effect of adding two types of dynamic dissipative mechanisms (thermal dissipation and a rate-type viscosity) to a stress with strain gradient. We perform numerical simulations to examine the behavior of these models under cyclic loading. Our main results are as follows.

- We find the two mechanisms induce similar hysteresis effects. They display stress-strain hysteresis loops whose size increases with the frequency of the loading function. The size of the loop is limited by the peaks and valleys of the nonmonotone local stress-strain law.

- Despite similar global behavior as described by hysteresis loops, there are significant differences in the local behavior of the models including stability of the center (Austenite) well at temperatures close to transition and the nucleation of phase transitions at this temperature.

- We also find that adding small material inhomogeneities to certain problems can stabilize numerical computation of solutions. We discuss the relationship of these numerical experiments with some similar analytic results.

1.1 Balance laws

We begin by introducing a model that includes a couple stress and both of the dynamic dissipative effects we wish to study (thermal and viscous). We consider

a bar of unit length and let $u(x,t)$ represent the longitudinal displacement and $\theta(x,t)$ the average absolute temperature at time $t \in [0, \infty)$ of the cross section of the bar with reference position $x \in [0, 1]$. We consider the following form of the balance of linear momentum.

$$\rho u_{tt} = \sigma_x + \nu u_{xxt} - \mu_{xx}.\tag{1}$$

Here $\rho > 0$ represents the uniform density of the bar, σ the stress under uniform deformation, $\nu > 0$ the viscosity coefficient, and μ the couple stress. The balance of energy takes the form

$$\rho e_t + q_x - \sigma u_{xt} - \mu u_{xxt}.\tag{2}$$

Here e denotes the specific internal energy and q the heat flux.

1.2   Constitutive assumptions

We use Fourier's law to describe the heat flux

$$q = -\kappa \theta_x,\tag{3}$$

with $\kappa > 0$. We introduce the specific free energy $\tilde{F}(u_x, u_{xx}, \theta, x)$ and define

$$\sigma := \rho \frac{\partial \tilde{F}}{\partial u_x},\tag{4}$$

$$\mu := \rho \frac{\partial \tilde{F}}{\partial u_{xx}},\tag{5}$$

and

$$e := \tilde{F} + \theta s\tag{6}$$

where

$$s := -\frac{\partial \tilde{F}}{\partial \theta}\tag{7}$$

is the specific entropy. We note that under these assumptions the Clausius-Duhem inequality holds

$$\rho s_t \geq -\left(\frac{q}{\theta}\right)_x.$$

In our numerical experiments we consider a free energy density of the form

$$\tilde{F}(u_x, u_{xx}, \theta, x) = \tilde{F}_0(\theta) + G(u_x, \theta) + \frac{\delta}{2} u_{xx}^2,\tag{8}$$

where

$$G(u_x, \theta) = \frac{\gamma}{2}(\theta - \theta_0)u_x^2 - \frac{\beta}{4}u_x^4 + \frac{\alpha}{6}u_x^6.\tag{9}$$

Here α, β, and γ are material constants. The temperature θ_0 is the critical value below which the uniform strain $u_x = 0$ (which one can think of as "Austenite") is unstable. We have included a Ginzburg or capillarity term in the form of $\frac{\delta}{2}u_{xx}^2$. The function $\tilde{F}_0$ is assumed to have the form

$$\tilde{F}_0(\theta) = c_e\theta\left(1 - \log\left(\frac{\theta}{\tilde{\theta}}\right)\right)$$

where c_e is the specific heat and $\tilde{\theta}$ is a material constant.

Under these assumptions, our balance laws become

$$\begin{aligned}\rho u_{tt} &= (\gamma(\theta - \theta_0)u_x - \beta u_x^3 + \alpha u_x^5)_x + \nu u_{xxt} - \delta u_{xxxx} \\ c_e\theta_t &= \kappa\theta_{xx} + \gamma\theta u_x u_{xt}.\end{aligned} \tag{10}$$

1.3   Boundary conditions

The bar will be dynamically loaded

$$\begin{aligned}u(0,t) &= 0 & (11) \\ u(1,t) &= m(t) & (12)\end{aligned}$$

where $m(t)$ is a periodic loading function. We prescribe vanishing strain gradients on the boundary

$$u_{xx}(0,t) = u_{xx}(1,t) = 0. \tag{13}$$

Boundary conditions for the temperature are an insulated left end and a radiating right end. These are given by

$$\begin{aligned}\theta_x(0,t) &= 0 & (14) \\ -\kappa\theta_x(1,t) &= \bar{\kappa}(\theta(1,t) - \theta_\Gamma). & (15)\end{aligned}$$

Here $\bar{\kappa}$ is the heat transfer coefficient and θ_Γ is the exterior temperature.

In [7], Bubner and Sprekels proved the existence of a unique classical solution to the system without viscosity effects ($\nu = 0$) such that θ remains positive for any time $T > 0$.

2   Numerical calculations on the system with thermal effects

In [8], Bubner used numerical simulations to study the system without viscosity effects ($\nu = 0$). In these experiments cubic spline finite elements are used to discretize the spatial derivatives. The weak formulation of the system is discretized with respect to the time derivative in such a way as to decouple the two balance equations. The discretized version of the balance of momentum is

solved first, followed by the discretized version of balance of energy. The non-linear terms in G are approximated by using a method developed by Niezgódka and Sprekels [18] for similar phase transition model. The resulting nonlinear equation is solved using a Newton method.

Bubner obtained values for the parameters $\alpha, \beta, \gamma, \delta$ and θ_0 from the experiments performed by Glasauer [13] on CuZnAl crystals. The values for ρ and c_e are taken from [11]. The value for κ is taken from [16] and $\bar{\kappa}$ is chosen as large as necessary to simulate a bath at the right boundary. In summary, the parameters are:

$$\alpha = 2.49 \cdot 10^8 \frac{J}{cm^3} \qquad \rho = 8.23 \frac{g}{cm^3}$$

$$\beta = 2.343 \cdot 10^6 \frac{J}{cm^3} \quad c_e = 3.1274 \frac{J}{cm^3 K}$$

$$\gamma = 190.18 \frac{J}{cm^3 K} \qquad \kappa = 2.39 \frac{W}{cm\ K}$$

$$\delta = 1 \frac{J}{cm} \qquad\qquad \bar{\kappa} = 10^9 \frac{W}{cm^2 K}$$

$$\theta_0 = 348.75 K.$$

For each of our simulations, we have a constant initial temperature θ_0 throughout the entire bar. The temperature surrounding the bar is $\theta_\Gamma = 373.1 K$. This temperature places the center (Austenite) well slightly below the two outer wells.

The initial displacement is chosen to be

$$u(x, 0) = \begin{cases} 0.09x & 0 \leq x < 0.25 \\ 0.045 - 0.09x & 0.25 \leq x < 0.75 \\ -0.09 + 0.09x & 0.75 \leq x \leq 1 \end{cases}, \qquad (16)$$

that is, the bar is initially in the phases corresponding to the outer wells. The loading function $m(t)$ consists of five equal lengths over the total time, T:

$$m(t) = \begin{cases} \frac{0.45}{T}t & 0 \leq t < \frac{T}{5} \\ 0.18 - \frac{0.45}{T}t & \frac{T}{5} \leq t < \frac{3T}{5} \\ -0.36 + \frac{0.45}{T}t & \frac{3T}{5} \leq t \leq T \end{cases}. \qquad (17)$$

In Figure 1, the strain u_x is plotted with respect to x and t with $T = 2sec$. At $t = 0$ there are two phase boundaries. These boundaries move towards each other as the rod is extended until the entire bar is in the phase corresponding to the right outer well of our three well potential. As the rod is pushed in the opposite direction, a single phase boundary between the right outer well to the left outer ("Martensite") well propagates from the right side of the rod to the left side. This phase transition is reversed when the rod begins to expand again.
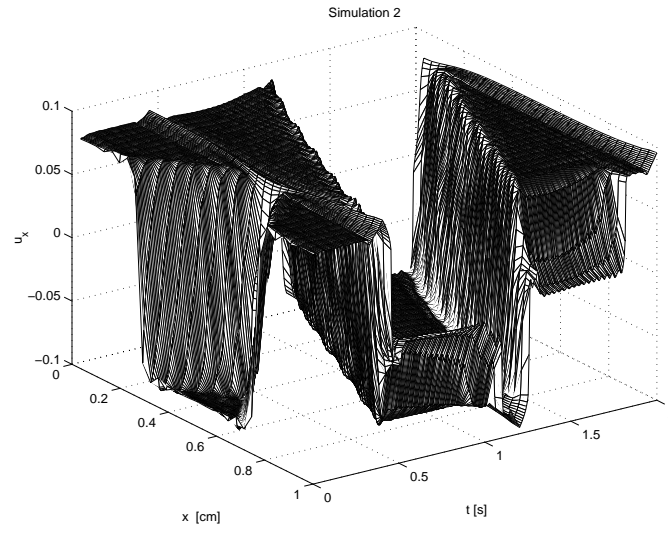
Figure 1: Calculated strain in a system with thermal dissipation. Piecewise linear periodic displacement loading at one end. Initial condition has two interfaces, but a single interface is seen after a "training" period.
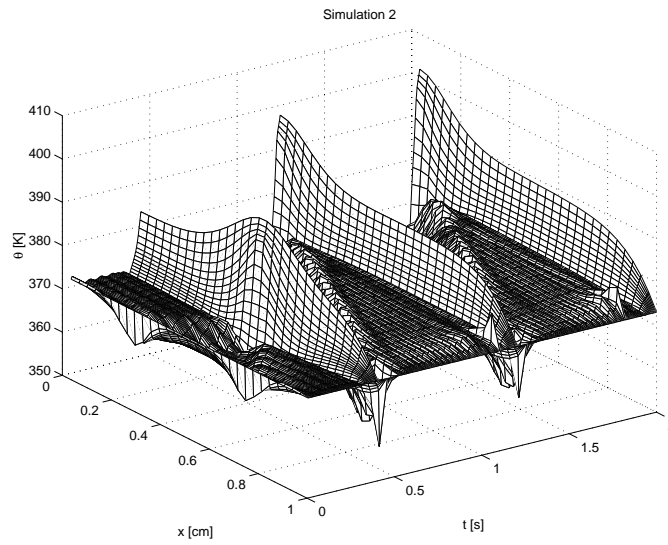

Figure 2: Simulation 4. Temperature, θ, vs x and t.

Note that despite the fact that we have chosen an ambient temperature at which the Austenite ($u_x = 0$) well lies below the outer Martensite wells, the simulation shows phase transitions between the two outer wells with no significant portion of the bar in the Austenite phase. This was discussed extensively in [8]. The phenomenon is attributed to a decrease in temperature at the point of phase transition as the strain goes over an energy barrier and kinetic energy is converted briefly to potential energy (see Figure 2).

Hysteresis curves for these experiments are examined below.

3   The system with prescribed thermal effects

3.1   The reduced system

We wish to compare the thermal dissipative mechanisms of the last section with a rate-type viscosity. To do this we consider a system in which thermal effects are "ignored." In this model we make two assumptions.

- We think of the temperature as a fixed, prescribed function $\hat{\theta}(x)$. Most authors assume the temperature to be constant. As we note below, there are good reasons to allow for more general prescribed distributions.

- We ignore the balance of energy equation. (Alternately, we could assume the existence of an external heat supply so that it is satisfied identically, but this seems a bit precious.)

Under these assumptions the balance of momentum becomes

$$\rho u_{tt} = \left(\gamma(\hat{\theta}(x) - \theta_0)u_x - \beta u_x^3 + \alpha u_x^5\right)_x + \nu u_{xxt} - \delta u_{xxxx}. \tag{18}$$

Our numerical calculations are based on a transformed version of equation (18). We consider the case $\nu^2 > 4\delta$ (in which viscosity dominates capillarity) and define

$$\begin{aligned} v &:= u_t - \epsilon_2^2 u_{xx} \\ w &:= u_x \end{aligned}$$

where

$$\begin{aligned} \epsilon_1^2 &:= \frac{\nu}{2} - \sqrt{\frac{\nu^2}{4} - \delta} \\ \epsilon_2^2 &:= \frac{\nu}{2} + \sqrt{\frac{\nu^2}{4} - \delta}. \end{aligned}$$

Using this transformation, we consider the system

$$\begin{aligned} w_t &= v_x + \epsilon_1^2 w_{xx} \tag{19} \\ \rho v_t &= G_w(w, \hat{\theta}(x))_x + \epsilon_2^2 v_{xx}, \tag{20} \end{aligned}$$

where

$$G_w(w, \hat{\theta}) := \gamma(\hat{\theta} - \theta_0)w - \beta w^3 + \alpha w^5.$$

We choose the initial conditions

$$w(t_0, x) \quad = \quad w_0(x) \tag{21}$$

$$v(t_0, x) \quad = \quad v_0(x) \tag{22}$$

and boundary conditions

$$w_x(t, 0) = 0 \qquad w_x(t, L) = 0 \tag{23}$$

$$v(t, 0) = 0 \qquad v(t, L) = g(t), \tag{24}$$

where $g \in C(0, \infty)$ is a periodic forcing function and $w_0 : [0, L] \to \mathbb{R}$ and $v_0 : [0, L] \to \mathbb{R}$ are continuous.

3.2 Remarks about the effects of inhomogeneity

In conducting our numerical experiments on the temperature independent system, we repeatedly saw extreme instabilities when computing very "clean" problems (e.g. materially homogeneous problems starting from homogeneous initial conditions and with $\theta(x)$ held constant in (18)). We were unable to predict the number or location of nucleation of interfaces which could change drastically with small changes in the problem. These instabilities sometimes disappeared after a "training period" of several cycles.

Of course, this is not completely unexpected. The basic underlying problem (minimizing a multiwell potential) is extremely unstable. For example, the problem of minimizing

$$\int_0^1 (1 - u_x^2)^2$$

subject to the boundary conditions $u(0) = u(1) = 0$ can be solved by taking *any* set $\mathcal{S} \subset [l, \infty]$ with measure $1/2$, setting $u'(x) = 1$ on $\mathcal{S}$ and $u'(x) = -1$ on it's complement. (Of course, the main goal of investigations such as this paper is to explore the effects of various "selection mechanisms" such as capillarity, viscosity, and thermal effects to determine their physical relevance.)

It was interesting, though, that these instabilities rarely occurred (and were much less pronounced when they did occur) in the simulations of the system with thermal effects and in some similar calculations performed on a system with an order parameter [17]. We were led to the conjecture that perhaps the material inhomogeneities introduced by the variations in the temperature or order parameter were stabilizing the system. The stabilizing effect of material inhomogeneity has been observed before. For example, James [15] showed that the effects of a gravitational body force on an otherwise homogeneous bar under a dead load results in absolutely stable solutions with at most one phase boundary. Without the gravitational force, there exists an infinite family of solutions
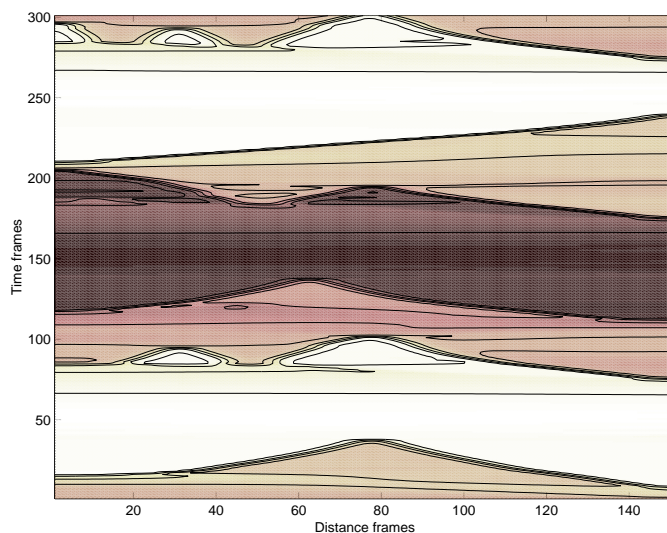
Figure 3: Simulation of a materially homogeneous system with rate-type viscosity and no temperature effects. Contour plot of u_x with loading function $g(t) = 0.09 \sin(2\pi t)$. Note the multiple phase boundaries that persist in the solution.

with the number of phase boundaries unlimited. More generally, discussions of the physics of hysteresis often revolve around "dirt," "inclusions", "pinning" and other effects of material inhomogeneity. Unfortunately, the mathematical problems we consider are often too "clean" to reflect this physics.

In the case of our system without thermal effects, we found that by introducing inhomogeneities using a prescribed temperature with small spatial variations we were able to eliminate almost all of the instabilities in the homogeneous problem. For example, in Figure 3 we observe a simulation of a homogeneous bar with homogeneous initial conditions. Our simulation shows solutions with an erratic nucleation of multiple phase boundaries. On the other hand, in Figure 4 we show a simulation under the same conditions except that we have introduced a fixed variation in the specified temperature of 1° about 373.1° Kelvin. We see a much more regular pattern, with a single interface selected.

3.3   Numerical Simulations

In [17], Mackin used numerical simulations to study a Gurtin-Fried type model for solid-solid phase transition in one space dimension including an order parameter. Eliminating the order parameter in this model results in the system with prescribed thermal effects (19) and (20). An outline of the Crank-Nikolson-Galerkin method applied to this system is as follows. Piecewise linear finite
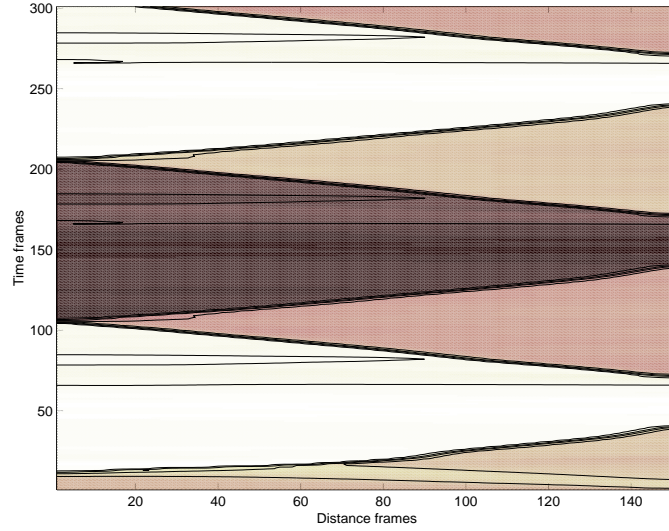
Figure 4: This figure shows the same model and boundary conditions as the previous figure, but with a small inhomogeneous perturbation in the constitutive function. Note that this slight inhomogeneity stabilizes a solution with a single phase transition.

elements are used to discretize the x derivatives. The weak formulations of the system is then discretized symmetrically about $t_{n-\frac{1}{2}}$ with respect to the t derivatives. The nonlinear terms are linearized using the previous two time steps, necessitating a predictor/corrector method to initialize the algorithm.

We use the values of $\alpha, \beta, \gamma, \rho$ and θ_0 listed in (2). We also choose $\epsilon_1^2 = 1\dfrac{cm^2}{sec}$ and $\epsilon_2^2 = 1\dfrac{g}{cmsec}$ to reflect the previous choice of $\delta = 1$ in Section 2, which in turn implies that $\nu = 2\dfrac{g}{cmsec}$. For each of our simulations, we have the initial state $w(x,0) = u_x(x,0)$ where $u(x,0)$ is defined in (16). The loading function is also the same, that is, $v(1,t) = g(t) = m'(t)$, where $m(t)$ is defined in (17).

We define a fictitious temperature, θ, as a function of x by

$$\theta(x) = \theta_1 + \xi \sin(6\pi x).$$

The role of this function is simply to place a small material inhomogeneity in our constitutive functions. As described in the previous section, the homogeneous bar($\xi = 0$) exhibits multiple phase transitions that are not stable with respect to small perturbations in ξ. Introducing slight variations in θ by setting $\xi = 1°$ results in stable single phase transitional solutions for u_x, see Figure 5, and we have used this material inhomogeneity in our hysteresis calculations below.
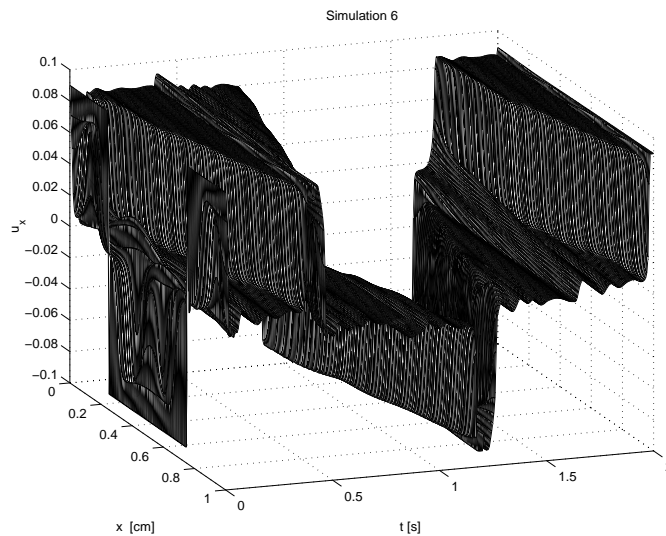
Figure 5: Strain calculated for the system with rate-type viscosity with small material inhomogeneity.

4   Comparison of the Two Models

In some ways, solutions of the system with rate-type viscosity and no temperature effects have much the same behavior as the system with thermal dissipation: both systems favor single phase transitions between regions of essentially constant strain. However, we can observe a few significant differences.

- While the model with thermal dissipation exhibited transitions between the two Martensite wells, the model with rate-type viscosity displays phase transitions between Austenite and one of the Martensite wells depending on the applied load. The latter behavior is far more in keeping with a quasistatic analysis. A phase plane analysis similar to that of Carr, Gurtin, and Slemrod [9] shows, that in the ambient temperature range we consider, the only solutions to the steady-state problem have phase transitions between the center well and one of the outer wells, never between the two outer wells. This emphasizes that the dynamics of the thermal effects are responsible for the Martensite-Martensite transitions in Section 2.

- The nucleation of hysteresis was quite different in the simulations produced for this paper. In the model with thermal dissipation, phase transitions consistently nucleated at the right end ($x = 1$). This is the end at which the time-dependent displacement and the radiating temperature condition are placed. In contrast, the end at which the phase transition nucleates
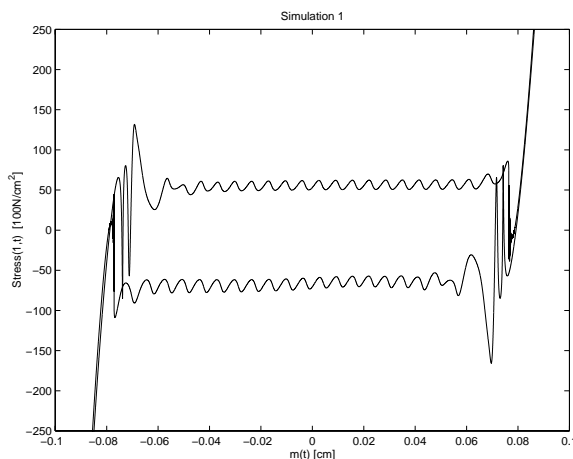
Figure 6: Right-end stress vs. right-end displacement for model with thermal dissipation. Simulation 1. Period of loading function: 0.5 sec.

alternates in the model with rate-type viscosity. While the radiating end condition is the most obvious difference between the boundary conditions of the two models, we have no analytic explanation for the difference in nucleation.

The hysteresis loops produced by the two models exhibited a similar dependence on rate.

- Systems loaded with a very long period (e.g. Figures 8 and 12) exhibit very little hysteresis, with stress-strain curves close to the Maxwell line. This is similar to the quasistatic calculations of [21, 22].

- For smaller periods, faster loading, the hysteresis loops grow. For the smallest periods we calculate, the loops are close to the width that would be described by the local maximum and minimum values of the uniform stress-strain function $\frac{\partial G}{\partial u_x}$. However, at this point inertial effects begin to cause the hysteresis loop to break up.
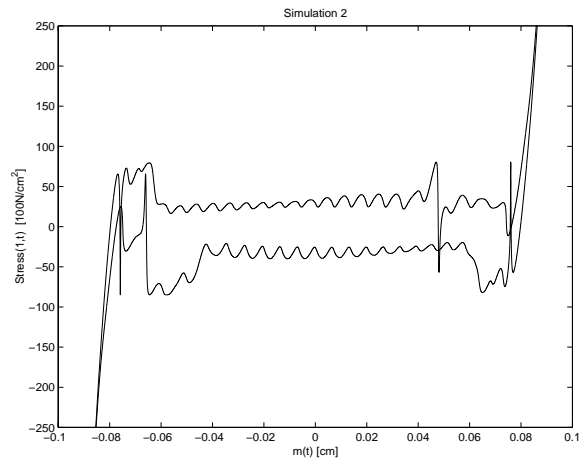
Figure 7: Right-end stress vs. right-end displacement for model with thermal dissipation. Simulation 2. Period of loading function: 2 sec.
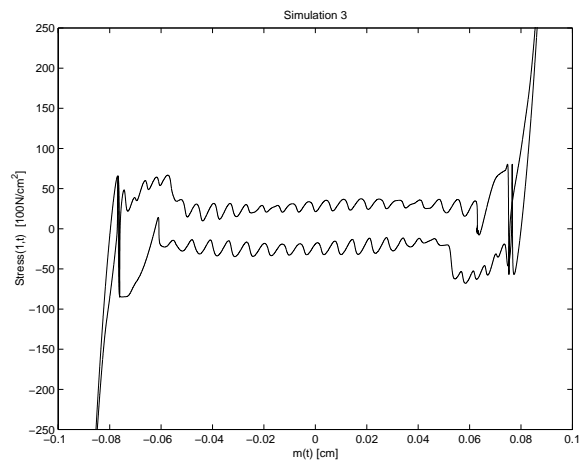

Figure 8: Right-end stress vs. right-end displacement for model with thermal dissipation. Simulation 3. Period of loading function: 4 sec.
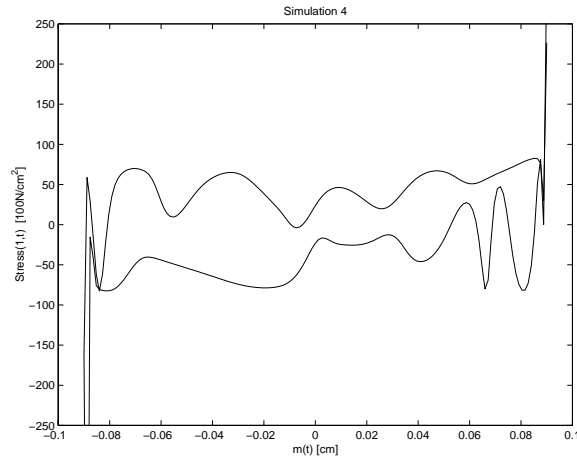
Figure 9: Right-end stress vs. right-end displacement for model with rate-type viscosity. Simulation 4. Period of loading function: 0.5 sec.
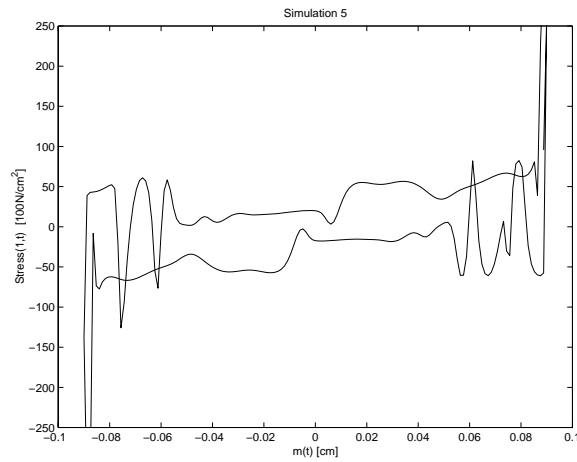

Figure 10: Right-end stress vs. right-end displacement for model with rate-type viscosity. Simulation 5. Period of loading function: 1.0 sec.
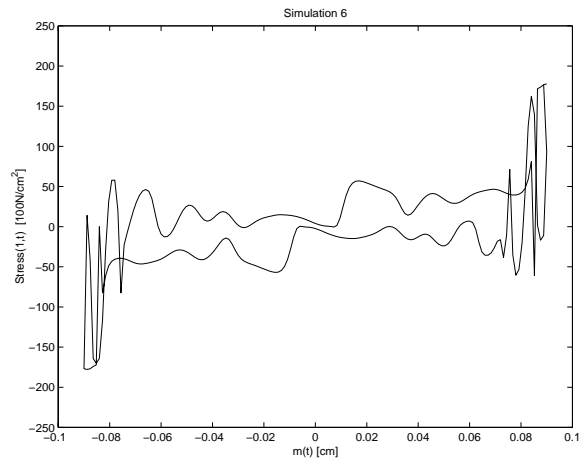
Figure 11: Right-end stress vs. right-end displacement for model with rate-type viscosity. Simulation 6. Period of loading function: 2.0 sec.
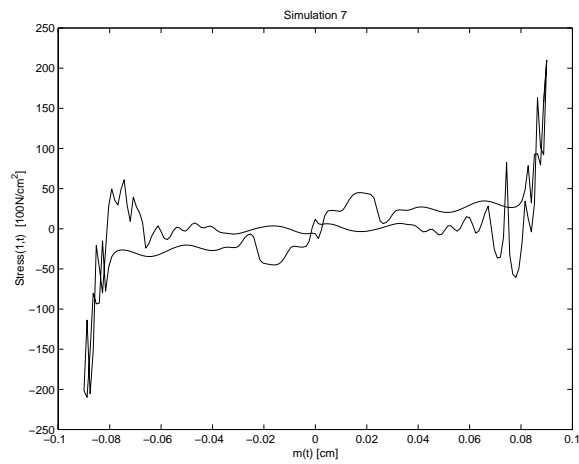

Figure 12: Right-end stress vs. right-end displacement for model with rate-type viscosity. Simulation 7. Period of loading function: 4.0 sec.

Simulation	Period	Average Width of Hysteresis	Model
1	0.5	123	Thermal dissipation
2	2	70	Thermal dissipation
3	4	66	Thermal dissipation
4	0.5	110	Rate-type viscosity
5	1	85	Rate-type viscosity
6	2	51	Rate-type viscosity
7	4	27	Rate-type viscosity

Table 1: Width of hysteresis as a function of loading period. Loading functions are piecewise linear.

References

[1] C. Abeyaratne, C. Chu, and R.D. James. *Kinetics and hysteresis in martensitic single crystals.* 1994.

[2] C. Abeyaratne and J.K. Knowles. A continuum model of a thermodynamic solid capable of undergoing phase transitions. *J. Mech. Phys. Solids*, 41:541–571, 1993.

[3] J.M. Ball, C. Chu, and R.D. James. Hysteresis during stress-induced variant rearrangement. *Journal de Physique*, 5(8), 1995.

[4] J.M. Ball, P.J. Holmes, R.D. James, R.L. Pego, and P.J. Swart. On the dynamics of fine structure. *J. Nonlinear Sci.*, 1:17–70, 1991.

[5] D. Brandon, T. Lin, and R.C. Rogers. Phase transitions and hysteresis in nonlocal and order parameter models. *Meccanica*, 30:541–565, 1995.

[6] M. Brokate and J. Sprekels. Optimal control of thermomechanical phase transitions in shape memory alloys: Necessary conditions of optimality. *Mathematical Methods in the Applied Sciences*, 14:265–280, 1991.

[7] N. Bubner and J. Sprekels. Optimal control of martensitic phase transitions in a deformation-driven experiment on shape memory alloys. *Advances in Mathematical Sciences and Applications*, 8(1):299–325, 1998.

[8] Nikolaus Bubner. Landau-ginzburg model for a deformation-driven experiment on shape memory alloys. *Continuum Mechanics and Thermodynamics*, 8:293–308, 1996.

[9] Jack Carr, Mortin E. Gurtin, and Marshall Slemrod. Structured phase transitions on a finite interval. *Archives of Rational Mechanics and Analysis*, 86(4):317–351, 1984.

[10] J.L. Ericksen. Equilibrium of bars. *J. of Elasticity*, 5(3/4):191–201, November 1975.

[11] S. Fu, Y. Huo, and I. Müller. Thermodynamics of pseudoelasticity - an analytical approach. *Acta Mechanica*, 99:1–19, 1993.

[12] S. Fu, I. Müller, and H. Xu. The interior of the pseudoelastic hysteresis. *Mat. Res. Soc. Symp. Proc.*, 246:39–42, 1992.

[13] U. Glasauer. Dissertation TU Berlin.

[14] S. Hou and I. Müller. Nonequilibrium thermodynamics of pseudoelasticity. *Continuum Mech. Thermodyn.*, 5:163–204, 1993.

[15] Richard D. James. Co-existent phases in the one-dimensional static theory of elastic bars. *Archives of Rational Mechanics and Analysis*, 72:99–140, 1979.

[16] O. Klein. Stability and uniqueness results for a numerical approximation of the thermomechanical phase transitions in shape memory alloys. *Advances in Mathematical Sciences and Applications*, 5:91–116, 1995.

[17] Gail Mackin. On an order-parameter model of solid-solid phase transition. *Ph.D. Thesis, Virginia Polytechnic Institute and State University*, 1997.

[18] M. Niezgodka and J. Sprekels. Convergent numerical approximations of the thermomechanical phase transitions in shape memory alloys. *Numerical Mathematics*, 58:759–778, 1991.

[19] R.C. Rogers and L. Truskinovsky. Discretization and hysteresis. *Physica B*, 233:370–375, 1997.

[20] L. Truskinovsky. Transition to detonation of dynamic phase changes. *Archives of Rational Mechanics and Analysis*, 125:375–397, 1994.

[21] A. Vainchtein, T.J. Healy, P. Rosakis, and L. Truskinovsky. The role of the spinodal region in one-dimensional martensitic phase transitions. *Physica D*, 115:29–48, 1998.

[22] A. Vainchtein and P. Rosakis. Hysteresis and stick-slip motion of phase boundaries in dynamic models of phase transitions. *To appear in J. Nonlinear Sci.*, (1999).